Lab on a Chip

RSC Publishing

PAPER

View Article Online
View Journal

Quantitative probing of surface charges at dielectric–electrolyte interfaces†

Cite this: DOI: 10.1039/c3lc41351a

Weihua Guan,[a] Nitin K. Rajan,[b] Xuexin Duan[a] and Mark A. Reed*[ab]

Received 9th December 2012,
Accepted 31st January 2013

DOI: 10.1039/c3lc41351a

www.rsc.org/loc

The intrinsic charging status at the dielectric–electrolyte interface (DEI) plays a critical role for electrofluidic gating in microfluidics and nanofluidics, which offers opportunities for integration of wet ionics with dry electronics. A convenient approach to quantitatively probe the surface charges at the DEI for material pre-selection purpose has been lacking so far. We report here a low-cost, off-chip extended gate field effect transistor configuration for direct electrostatic probing the charging status at the DEI. Capacitive coupling between the surface charges and the floating extended gate is utilized for signal transducing. The relationship between the surface charge density and the experimentally accessible quantities is given by device modeling. The multiplexing ability makes measuring a local instead of a globally averaged surface charge possible.

Introduction

Analogous to field effect modulation of the surface potential in metal-oxide semiconductor field effect transistors (MOSFETs), the potential at the dielectric–electrolyte interface (DEI) in microfluidic and nanofluidic systems can be tuned in a similar fashion, enabling various lab-on-chip applications. This so called electrofluidic gating[1] approach leverages both the structural and functional properties of MOSFETs, offering opportunities for seamlessly integrating wet ionics with dry electronics. However, most of the channel-forming dielectric materials will spontaneously obtain surface charges when brought into contact with an aqueous phase electrolyte. These intrinsic surface charges function similarly to the surface states in semiconductors. Therefore, the surface charge density at the DEI is one of the most important parameters for effective electrofluidic gating.[2,3] Though electrostatic force microscopy (EFM) has been utilized to probe the surface charges in aqueous solutions,[4] it requires bulky instrumentation and a quantitative measurement is difficult. In the nanofluidic platform, the conventional method to derive the surface charge density information at the DEI is by plotting the nanochannel conductance against ionic concentrations on a log–log scale. The surface charge can be extracted from the plateau in that plot at the low ionic concentration region where surface charge dominates the ionic transport.[5–7] This approach is quite suitable for characterizing the nanochannel after its formation. Nevertheless, it becomes rather inconvenient and tedious to examine various channel-forming dielectric materials beforehand. A faster and simpler method is desirable for such a material pre-selection purpose.

Direct charge detection by field effect has been the scaffold for various FET based biosensors since the invention of the ion selective field effect transistor (ISFET).[8] The problem of using a conventional ISFET configuration for the above-mentioned material pre-selection purpose is multifold. The most severe one is the reliability issues due to the direct contact of the electrolytes with the FETs. An extended gate structure, where the sensing area is placed away (either laterally or vertically) from the active region of on-chip integrated FETs, has been widely adopted to solve the chemical contamination problem.[9] Though successful, the extended gate structure with on-chip FETs is ill-suited for the channel-forming material pre-selection purpose due to the following reasons. First, the transistors cannot be repeatedly used because dielectric materials cannot be easily removed once deposited. Second, the sample preparation is time-consuming since it involves a complex CMOS fabrication process. Third, common FET based sensors require a liquid filled reference electrode, such as a saturated calomel electrode or Ag/AgCl electrode, to set the potential of the electrochemical system. Such a reference electrode cannot be easily integrated in a standard CMOS process, preventing the realization of really low-cost, disposable devices for material pre-selection purpose.

Here, we report an off-chip extended gate (OCEG) architecture for directly probing the surface charges at the DEI, getting rid of most of the aforementioned problems in the on-chip extended gate structures. Capacitive coupling between surface charges at the DEI and a floating gate is utilized for signal transduction. Successful quantitative local surface

[a]Department of Electrical Engineering, Yale University, New Haven, Connecticut 06520, USA
[b]Department of Applied Physics, Yale University, New Haven, Connecticut 06520, USA. E-mail: mark.reed@yale.edu

† Electronic supplementary information (ESI) available. See DOI: 10.1039/c3lc41351a

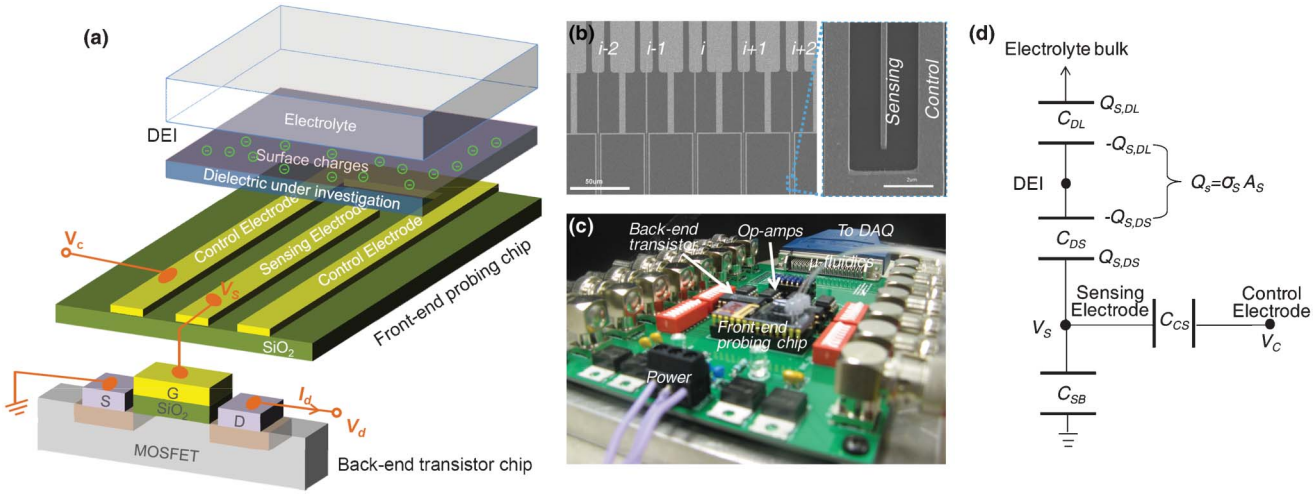

Fig. 1 (a) Schematic of the off-chip extended gate configuration. It consists of two independent parts: a disposable front-end probing chip and a reusable back-end sensing transistor chip. The dielectric material under investigation is deposited on top of the front-end chip by any necessary means. Surface charges developed at the dielectric–electrolyte interface (DEI) capacitively modulate the potential of the floating sensing electrode (V_S) underneath and thus the drain current in the back-end transistors. (b) Scanning electron microscope (SEM) of the fabricated front-end probing chip, which consists of an array of sensing/control electrode sets. The magnified SEM image shows a single sensing electrode and its corresponding control electrode. (c) Photograph of the printed circuit board (PCB) setup. The front-end probing chip is used in a plug-and-play fashion. The whole setup is placed in a Faraday cage to shield the electrostatic noise. (d) The equivalent small signal circuit model of the system. The total amount of the surface charge Q_S is redistributed to the two parallel capacitors (C_{DL} and C_{DS}) according to the capacitor's ratio. The actual potential at the floating sensing electrode (V_S) is concurrently determined by both V_C and the surface charges developed at the DEI.

charge measurements are demonstrated by examining two most frequently used dielectric materials (silicon dioxide and silicon nitride) under various pH and ionic concentration conditions.

Device principle

Fig. 1a shows the schematic of the OCEG configuration. The front-end probing chips, containing an array of independent sensing and control electrodes, were massively manufactured by conventional lift off process (Fig. 1b). The front-end probing chip and the back-end sensing transistors are integrated on a single printed circuit board (PCB), accompanying signal amplification and data acquisition interface for personal computers (Fig. 1c). The modular configuration of a separate front-end probing chip and a back-end transistor chip has clear advantages in terms of cost and disposability. When electrolyte is brought into contact with the dielectric material under investigation, surface charges will develop at the DEI according to site-binding theory.[10] These surface charges capacitively affect the potential of the floating sensing electrode (V_S) underneath. This capacitive coupling process can be understood from a charging by induction picture. The presence of the surface charges at the DEI induces charge polarization in the conductive sensing electrode, which further produces an electric field across the gate oxide of the transistor, modulating the drain current accordingly. By measuring the drain current change, one can detect the charging status at the DEI.

To find out a quantitative and predictive dependence of the sensing electrode potential V_S on the surface charges, an equivalent small signal circuit model is developed, as shown in Fig. 1d. The total image charges induced by the surface charges are distributed into two capacitors, the electric double-layer capacitor, C_{DL}, and the capacitor between sensing electrode and DEI, C_{DS}. The amount of charges each capacitor obtains depends on the ratio of C_{DL} and C_{DS}. The induced charge on the sensing electrode ($Q_{S,DS}$) thus reads,

$$Q_{S,DS} = -\frac{C_{DS}}{C_{DS}+C_{DL}}\sigma_S A_s \quad (1)$$

where A_S is the overlapped area between the sensing electrodes and the electrolyte, and σ_S is the surface charge density at the DEI (the quantity of interest here).

Since the sensing electrode is electrically isolated, the total net charges within the sensing electrode must remain zero, unless a charge injection or ejection process (*e.g.*, tunneling) is involved. According to the charge conservation principle, we get the following relationship at the sensing electrode node in Fig. 1d,

$$Q_{S,DS} + (V_S - V_C)C_{CS} + V_S C_{SB} = 0 \quad (2)$$

where V_C is the voltage applied on the control electrode, C_{CS} is capacitor between the control and the sensing electrode. C_{SB} is the lumped capacitance between the sensing electrode and silicon body of MOSFET. Note that all voltages above are referenced with respect to potential in the silicon body, which is ground in this study.

By combining the eqn (1) and eqn (2), the potential at the sensing electrode can be written as,

$$V_S = \frac{A_s C_{DS}}{(C_{DS}+C_{DL})(C_{CS}+C_{SB})}\sigma_S + \frac{C_{CS}}{C_{CS}+C_{SB}}V_C \qquad (3)$$

Eqn (3) represents the relationship between the V_S, V_C and σ_S at the DEI. It states that the ultimate sensing electrode potential is a linear superposition of two independent contributions, the surface charges and the control electrode voltage. Indeed, the control electrode offers an extra degree of freedom in device operation by applying an independent V_C, which functions similarly as a capacitively coupled reference electrode in FET sensors.[11] The transistor's quiescent working point can be independently set by an appropriate V_C. The sensing transistor can thus be tuned to ensure maximum sensitivity. This principle is very similar to the chemoreceptive neuron MOS transistors[12] and the charge modulated FET sensors.[13]

To further relate the sensing electrode potential V_S with the experimentally accessible quality (*i.e.*, the drain current I_d), we note that the general form of the *I–V* characteristics of a MOSFET can be expressed as $I_d = f(V_{gs},V_{ds})$ for sub-threshold, linear and saturated region,[14] where V_{gs} equals the sensing electrode potential V_S, and V_{ds} is the drain voltage of the MOSFET. The I_d-V_{gs} curve at a constant V_{ds} could be tested thoroughly off-line before performing any surface charge measurements (ESI, Fig. S1†), serving as a look-up table for converting the measured drain current I_d back into V_S value (and thus the surface charge density, using eqn (3)) when carrying out the real surface charge measurements (ESI, Fig. S2†).

Materials and methods

Device fabrication

The front-end probing chips, containing independent sensing and control electrodes (50 nm Au with 10 nm of Cr as adhesive layer), were massively manufactured by conventional electron beam evaporation and lift off process on a 4 inch Si wafer with 3 μm-thick SiO_2 as isolating layer. Hybrid optical lithography and e-beam lithography was employed to ensure both low cost and high spatial resolution. After depositing the dielectric material of interest, the front-end probing chip was wire-bonded with a ceramic chip carrier. A PDMS based microfluidic system was adopted to deliver the electrolyte solution.

Materials

SiO_2 with thickness ranging from 73.8 nm to 168.5 nm and SiN_x with thickness ranging from 43 nm to 197.1 nm were deposited by plasma enhanced chemical vapor deposition (PECVD) at 400 °C. The reactive gases for depositing SiO_2 are silane (SiH_4) and nitrous oxide (N_2O). The reactive gases for depositing SiN_x are silane and ammonia (NH_3). The chamber pressure for both depositions is 2 Torr. The dielectric materials were sequentially cleaned (2 min each at room temperature) with acetone, methanol, and finally DI water before testing. The electrolyte we used is Dulbecco's Phosphate Buffered Saline (Catalog Number 14190-136, Invitrogen), the pH of which is adjusted by adding hydrochloric acid or potassium hydroxide into this buffer. The back-end sensing transistors are commercially available n-channel MOSFET with zero volt threshold voltage (ALD110800, Advanced Linear Devices).

Electrical measurement

The entire measurement procedure is done using an automated system at room temperature. The drain current for each sensing electrode, at a constant drain voltage (100 mV), is amplified with operational amplifiers (Op-amps) and recorded in a multiplexed fashion using an 8-channel data acquisition card (NI PXI-4224, National Instrument). The voltage on the control electrode is applied as 0 V to maximize the sensitivity. The whole testing system is housed inside a homemade light-shielding Faraday cage. This shielding is essential for a stable electric measurement since the bulk of the electrolyte is in a floating potential. We found that the whole testing system is extremely sensitive to the surrounding electrostatic environment (ESI movie†). The electrolyte with controlled ionic concentration and pH values was delivered by pumps (New Era Pump Systems, Inc.), controlled by a LabVIEW (National Instruments) program. The final drain current is obtained at least 10 min after the solution is brought into the DEI, even though it usually takes less than 1 min for the current to reach equilibrium (see the time course data in the ESI, Fig. S2†).

Results and discussion

Effect of pH on the surface charge density

To verify the validity of device principle, we first tested the pH effect on the surface charge at the DEI. According to the well-accepted site-binding model,[10] the dielectric surface has ionizable sites that react directly with the electrolyte to bind or release hydrogen ions. The surface therefore becomes more or less charged depending on the pH. As a demonstration of using the OCEG structure to probe charging status at the DEI, we measured the pH dependence of the sensing electrode potential at a constant ionic strength (0.001 × PBS buffer) for both SiO_2 and SiN_x samples and extracted σ_S based on eqn (3).

Fig. 2a show the measured sensing electrode potential as well as σ_S for SiO_2 at various pH conditions. The SiO_2/electrolyte interface becomes more negatively charged as the pH increases. When SiO_2 is in contact with an aqueous solution, it hydrolyzes to form surface silanol (SiOH) groups. The amphoteric nature of the silanol groups causes the variation of the oxide surface charge when varying the pH according to the reactions $SiOH_2^+ \rightleftarrows SiOH + H^+$ and $SiOH \rightleftarrows SiO^- + H^+$. Increasing the pH therefore results in a more negatively charged surface. The surface charge density at the SiO_2/PBS interface varies from -2.8 ± 0.7 mC m^{-2} to -13.7 ± 4.82 mC m^{-2} when changing pH from 5 to 9. In comparison, the surface charge density at the PECVD SiO_2/electrolyte interface, derived by plotting the nanochannel conductance against the

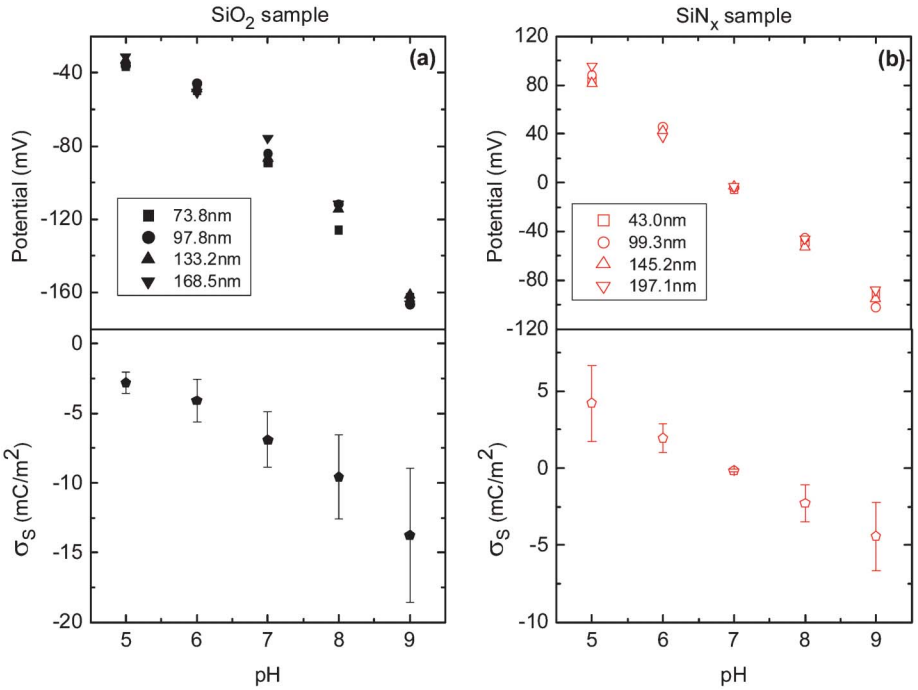

Fig. 2 Measured sensing electrode potential (upper panels) and the extracted surface charge density σ_S (averaged over the four thicknesses, lower panels) as a function of pH for (a) SiO_2 sample and (b) SiN_x sample. The measurement is performed at a constant ionic strength (0.001 × PBS solutions).

ionic concentrations on a log–log scale, is estimated to be −2 mC m^{-2} [3] at pH 7. The reasonable agreement between these two surface charge density measurement methods confirms the validity of our simple OCEG structure. The point of zero charge (pzc) of SiO_2 in the 0.001 × PBS solution is extrapolated to be around 4.27 ± 0.08 by linear fitting of the experimental data shown in Fig. 2a, which is a little higher than the pzc of typical silicon oxide material (~2–4).

Fig. 2b show the results for the SiN_x/PBS interface. A negative shift of the surface charge density as increasing the pH is also observed. However, the polarity of the surface charge is reversed at pH ~ 6.5, indicating the SiN_x deposited by our PECVD has a pzc around 6.5. The surface charge density at the SiN_x/PBS interface ranges from 4.21 ± 2.45 mC m^{-2} to −4.42 ± 2.2 mC m^{-2} when changing pH from 5 to 9. Silicon nitride is known to produce both a basic primary amine sites $SiNH_2$ ($SiNH_3^+ \rightleftarrows SiNH_2 + H^+$) and an amphoteric silanol sites.[15] The amphoteric silanol sites are from the oxidation of the silicon nitride surface. The primary amine sites $SiNH_2$ are expected to have a pK of around 10. Since the pzc of SiN_x sample has a value lower than 10, it can be assumed that all the amine sites are positively charged at the pzc of SiN_x sample. As a result, the silanol sites tend to donate a proton to the amine sites at most pH values. The pzc of SiN_x (pH 6.5) occurs at the pH where the negative charge on the silanol sites balances the fixed positive charge on the amine sites. The surface site theory can be used to calculate the ratio of the number of amine sites to silanol sites on the SiN_x/PBS interface:[16]

$$\frac{N^{NH_2}}{N^{OH}} = 2\sqrt{\frac{K_{a2}}{K_{a1}}}\sinh[2.303(pH_{pzc} - pH_{pzc}^{OH})] \quad (4)$$

where K_{a1} and K_{a2} are the surface equilibrium constants of the acid/base reactions of the amphoteric silanol sites, pH_{pzc} is the zero charge point for SiN_x sample and pH_{pza}^{OH} is the zero charge point for silanol sites only. A typical value[16] for the dissociation constants is 7 × 10^{-4}. Using the experimentally derived value of pH_{pzc}^{OH} as 4.27 and pH_{pzc} as 6.5, the ratio of N^{NH_2}/N^{OH} is calculated to be around 6%. It is therefore apparent that PECVD nitride surfaces are highly populated with silanol sites, instead of the amine sites. The tendency of SiN_x surfaces to oxidize has been shown extensively before.[17]

Surface charge extraction at different ionic concentrations

Having verified the capability of using OCEG architecture to quantitatively detect the surface charges, we carried out experiments on the influence of different ionic concentrations under a constant pH value (pH = 7) to further relate the experimentally accessible V_S with σ_S at arbitrary ionic strengths. Fig. 3 shows the measured floating sensing electrode potential V_S as a function of the PBS concentration for both SiO_2 and SiN_x materials. A clear increase of the absolute value of the V_S when decreasing the PBS buffer concentrations was observed. To understand this dependence and relate the surface charge density σ_S with the measured V_S under different ionic strength, we need to recall eqn (3). Since the control electrode potential applied is 0 V (see Experimental Section), the second term on the right hand side of eqn (3) can therefore be dropped. Moreover, it is reasonable to assume

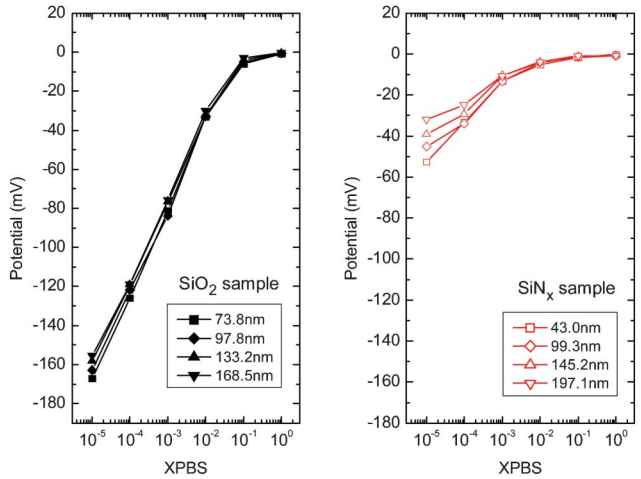

Fig. 3 Measured sensing electrode potential as a function of ionic strength for (a) SiO_2 with four different thicknesses and (b) SiN_x with four different thicknesses. Note that 1 × PBS corresponds to an ionic strength of about 150 mM. The pH is fixed at 7 for all data points.

$C_{SB} \gg C_{CS}$ in our devices, since the thickness of MOSFET gate oxide (50 nm) is much thinner than the distance between sensing and control electrode (>1 μm). Therefore, eqn (3) can be reduced to a simpler approximation form of,

$$V_S = \alpha \frac{A_s \sigma_S}{C_{SB}} \quad (5)$$

where $\alpha = (1 + C_{DL}/C_{DS})^{-1}$. It is easy to show that $C_{DL}/C_{DS} = \varepsilon_e t/\varepsilon_d \lambda_D$, where ε_e and ε_d is the relative permittivity of electrolyte and dielectric, respectively, and t and λ_D is the dielectric thickness and Debye length, respectively. At room temperature, one can consider in water the relation, $\lambda_D = 0.304/\sqrt{c}$, where λ_D is expressed in nanometers (nm) and c is the ionic strength expressed in molar (M).[18] Since 1 × PBS corresponding to an ionic strength around 150 mM, we therefore have $\lambda_D = 0.785/\sqrt{\mathrm{XPBS}}$. As a result, the factor α can be expressed as,

$$\alpha = (1 + 1.274 t\sqrt{\mathrm{XPBS}}\varepsilon_e/\varepsilon_d)^{-1} \quad (6)$$

where t is in nm. For a fixed dielectric thickness t, decreasing PBS concentrations will increase the factor α and thus increase the absolute value of the floating gate potential, consistent with the results shown in Fig. 3.

By fitting the experimentally derived PBS concentration *versus* V_S curve using the know parameters (C_{SB} = 12 pF and A_s = 1.4 × 10^{-8} m^2), it is possible to extract a value for σ_S. Table 1 shows the σ_S found by the least squares fitting for SiO_2 and SiN_x materials. The averaged surface charge density for SiO_2 is estimated to be −1.7 ± 0.492 mC m^{-2} and for SiN_x is −0.24 ± 0.0743 mC m^{-2} at pH 7. The lower surface charge density developed at the SiN_x surface than that of the SiO_2 surface can be understood from the different pzc value for PECVD SiO_2 (4.27) and PECVD SiN_x (6.5).

Another feature in Fig. 3 is that the measured sensing electrode potential (V_S) depends on the dielectric thickness and the dependency is more appreciable at low ionic strength. This can be understood from the dependence of factor α on the dielectric thickness t (eqn (6)). In the high ionic strength region, $1.274\sqrt{\mathrm{XPBS}}\varepsilon_e/\varepsilon_d >> 1$ and therefore α is less dependent on t, whereas in the low ionic strength region, $1.274\sqrt{\mathrm{XPBS}}\varepsilon_e/\varepsilon_d << 1$, and α shows a stronger dependence on t. This thickness dependence can also be understood from the physical picture that the total amount of the surface charge is redistributed to the two parallel capacitors (C_{DL} and C_{DS}) according to the capacitor's ratio (Fig. 1d) . At high ionic strength (small Debye length), the double layer capacitor C_{DL} is much larger than C_{DS} for all thicknesses, and therefore C_{DL} takes most of the charges and the measured sensing electrode potential is less dependent on the dielectric thickness. At low ionic strength (large Debye length), the double layer capacitor C_{DL} is comparable to or even smaller than C_{DS}, therefore the potential picked up from the sensing electrode is strongly dependent on C_{DS} (and thus the dielectric thickness).

Array implementation

Finally, the ability to quantitatively measure the surface charge density is not limited to a globally averaged value. The flexibility of the electrode patterning enables the multiplexed measurements for mapping out the spatially distributed localized surface charge. Fig. 4 shows measured spatial surface charge density by eight sensing electrodes on a same chip under various pH conditions. The sample under test is the 73.8 nm-thick SiO_2 and the electrolyte used is 0.001 × PBS. The distance between each sensing electrode (and therefore the lateral spatial resolution) is 40 μm (Fig. 1b). The localized surface charge densities can be determined by each electrode. For any pH values, the surface charge density shows a certain 'roughness', the variation coefficient of which is denoted as a percentage number, as shown in Fig. 4. The variation coefficient of surface charge densities probed by each sensing electrode is less than 10% in all pH conditions. Note that the variation coefficient is calculated as the ratio of the standard deviation to the mean value of all sensing electrodes. It is worth noting that the number of the sensing electrodes is not limited to eight channels. More electrodes with smaller electrode-to-electrode distance can lead to a finer mapping

Table 1 Surface charge density extracted by least squares fitting

Dielectric	Thickness (nm)	Fitted σ_S (mC m^{-2})	Dielectric	Thickness (nm)	Fitted σ_S (mC m^{-2})
SiO_2	73.8	−1.17	SiN_x	43.0	−0.144
	97.8	−1.47		99.3	−0.241
	133.2	−1.88		145.2	−0.288
	168.5	−2.30		197.1	−0.312

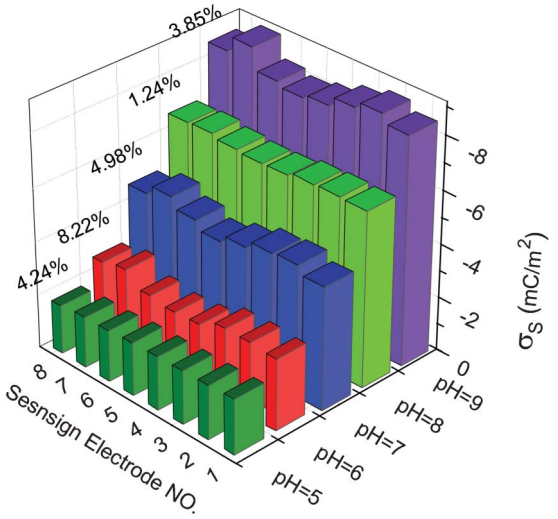

Fig. 4 Measured spatial surface charge distribution on a same chip (1 × 8 array) with various pH values. The dielectric material under investigation is the 73.8 nm-thick SiO_2 deposited by plasma-enhanced chemical vapor deposition (PECVD). The measurement is performed with a constant ionic strength at 0.001 × PBS solutions. The percentage number indicates the surface charge density variation coefficient (standard deviation/mean) over the eight channels.

of the surface charge distributions. Moreover, a two dimensional (2D) mapping of the surface charge distributions is possible by using 2D sensing electrodes with finer spatial resolution, using a similar technique as multielectrode arrays (MEAs).[19]

Conclusions

In summary, we have demonstrated a facile OCEG configuration for quantitatively probing the charging status at the dielectric–electrolyte interface for material pre-selection purposes. The use of the OCEG configuration allows the separation of wet ionics from dry electronics and completely eliminates reliability issues. The integrated control electrodes, which allows for adjusting a transistor's quiescent working point, offers an extra degree of freedom in device operation and circumvents the requirement for a bulky reference electrode. An analytical model to extract the surface charge density is developed. Experiments on two different dielectric materials have successfully demonstrated a reliable quantitative surface charge analysis. It is worth noting that even though the motivation here is to detect the charging status at the DEI, the OCEG architecture can be applied to any charge based sensing schemes (*e.g.*, biosensors).

Acknowledgements

We would like to thank Dr Yong Sun and Michael Power for the help during the device fabrication process. W.G. acknowledges the support from Howard Hughes Medical Institute International Student Research Fellowship. Facilities used were supported by Yale Institute for Nanoscience and Quantum Engineering and NSF MRSEC DMR 1119826.

References

1 Z. J. Jiang and D. Stein, *Langmuir*, 2010, **26**, 8161–8173.
2 R. Karnik, K. Castelino and A. Majumdar, *Appl. Phys. Lett.*, 2006, **88**, 123114.
3 W. H. Guan, R. Fan and M. A. Reed, *Nat. Commun.*, 2011, **2**, 506.
4 S. H. Xu and M. F. Arnsdorf, *Proc. Natl. Acad. Sci. U. S. A.*, 1995, **92**, 10384–10388.
5 D. Stein, M. Kruithof and C. Dekker, *Phys. Rev. Lett.*, 2004, **93**, 035901.
6 R. B. Schoch and P. Renaud, *Appl. Phys. Lett.*, 2005, **86**, 253111.
7 C. H. Duan and A. Majumdar, *Nat. Nanotechnol.*, 2010, **5**, 848–852.
8 P. Bergveld, *Sens. Actuators, B*, 2003, **88**, 1–20.
9 J. Vanderspiegel, I. Lauks, P. Chan and D. Babic, *Sens. Actuators*, 1983, **4**, 291–298.
10 D. E. Yates, S. Levine and T. W. Healy, *J. Chem. Soc., Faraday Trans. 1*, 1974, **70**, 1807–1818.
11 S. Chen and S. L. Zhang, *Anal. Chem.*, 2011, **83**, 9546–9551.
12 B. C. Jacquot, C. Lee, Y. N. Shen and E. C. Kan, *IEEE Sens. J.*, 2007, **7**, 1429–1434.
13 M. Barbaro, A. Bonfiglio and L. Raffo, *IEEE Trans. Electron Devices*, 2006, **53**, 158–166.
14 S. M. Sze, *Physics of Semiconductor Devices*, John Wiley and Sons, 1981.
15 D. L. Harame, L. J. Bousse, J. D. Shott and J. D. Meindl, *IEEE Trans. Electron Devices*, 1987, **34**, 1700–1707.
16 L. Bousse and S. Mostarshed, *J. Electroanal. Chem.*, 1991, **302**, 269–274.
17 H. Barhoumi, A. Maaref and N. Jaffrezic-Renault, *Langmuir*, 2010, **26**, 7165–7173.
18 J. N. Israelachvili, *Intermolecular and Surface Forces*, Academic Press, 2011.
19 P. Thiebaud, N. F. deRooij, M. KoudelkaHep and L. Stoppini, *IEEE Trans. Biomed. Eng.*, 1997, **44**, 1159–1163.

Supplementary Figure

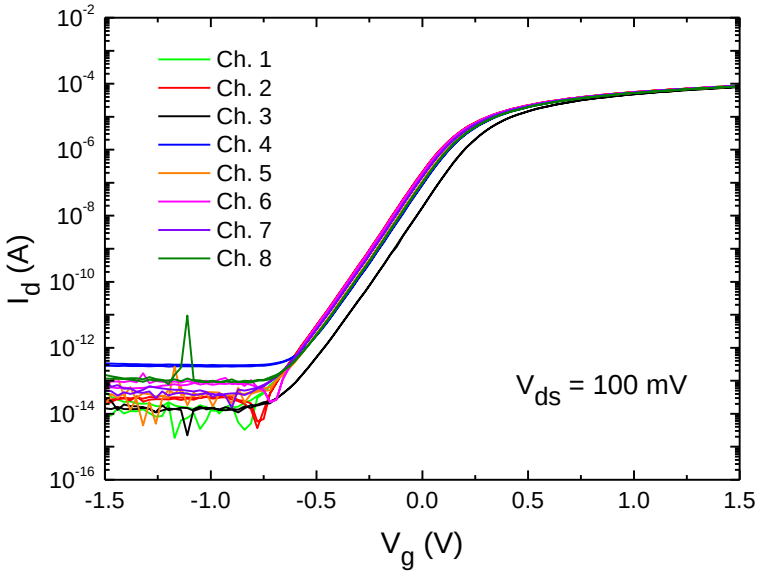

Supplementary Figure S1 | Back-end MOSFETs characterizations. The Drain to source voltage is held at 0.1 V. This curve serves as a look-up table for converting the measured drain current into the floating sensing electrode potential (V_S).

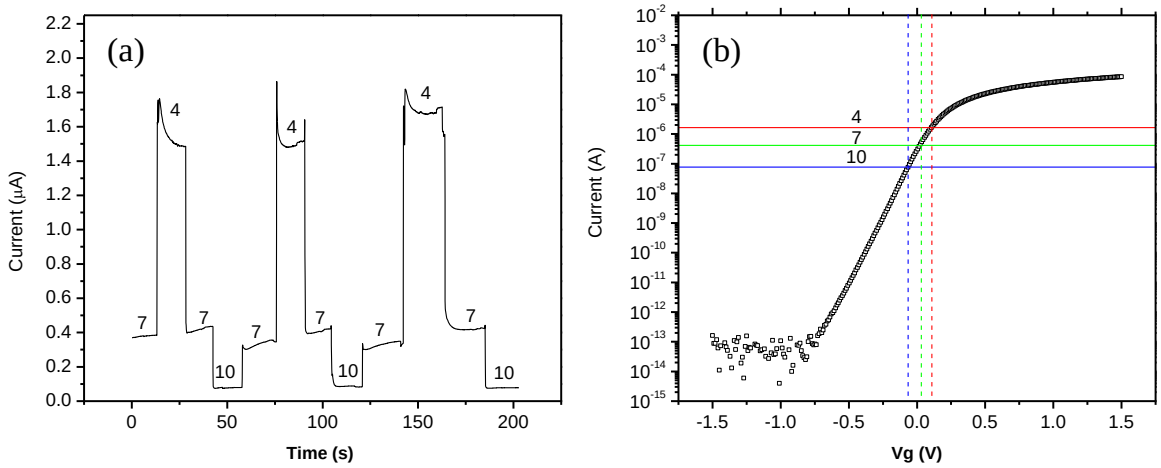

Supplementary Figure S2 | Methods to extract the floating sensing electrode potential (V_S) from the measured I_d value at various electrolyte condictions. (a) Time course of the drain current I_d for SiN_x sample under various pH conditions. (b) Procedures to find the corresponding floating sensing electrode potential at various pH conditions. Each drain current baseline is used to extract V_S by using the I_d-V_{gs} curve tested off-line before performing any surface charge measurements.

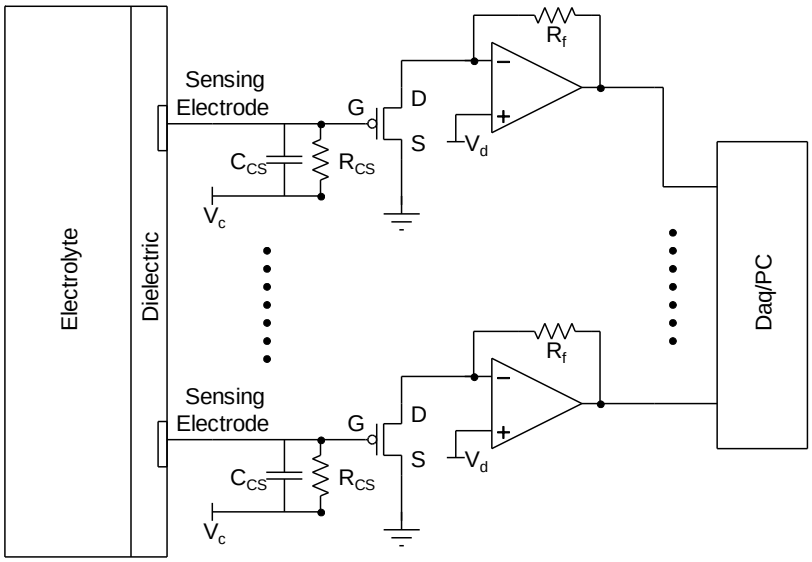

Supplementary Figure S3 | Schematic of the readout circuit for probing the charging status at the dielectric-electrolyte interface.

Supplementary Movie

The supplementary movie shows the response of the testing system to a moving hand around. The whole testing system is extremely sensitive to the electrostatic environment around. Therefore, it is essential to place the whole testing system inside a Faraday cage for a reliable electric measurement of the surface charge developed at the dielectric/electrolyte interface.